Proceedings of Global Power and Propulsion Society
ISSN-Nr: 2504-4400
GPPS Xi'an21
18th – 20th October, 2021
www.gpps.global

GPPS-TC-2021-179

THERMAL ANALYSIS OF HIGH SPEED ROLLER BEARING BASED ON PARTIAL POWER LOSS PREDICTION

Ying Pan
Northwestern Polytechnical University
panying000@yeah.net
Xianan, Shannxi, China

Wenjun Gao
Northwestern Polytechnical University
gaowenjun@nwpu.edu.cn
Xianan, Shannxi, China

Kun li
Northwestern Polytechnical University
likunkelly@163.com
Xianan, Shannxi, China

ABSTRACT

In the operation of rolling element bearings(REBs), lack of a more complete understanding of the thermal characteristics severely limits its reliability. In this paper, an ananalytical approach is presented to combine the thermal network method with partial power loss prediction, to obtain a more precise thermal analysis of REBs. Bearing elements, including the inner and outer rings, the rollers and the cage, were represented by hundreds of finite-element nodes, and a thermal network was built based on their heat transfer relationship. Friction losses in different contact zones of the bearing were calculated by solving a quasi-dynamic model, which were added to the nodes in the contact zones as their heat source. By comparing with experimental results, the error of predicted temperature of the surface centerline of outer ring is less than 13%, indicating that the method developed in this paper is reliable enough for roller bearing's thermal analysis.

INTRODUCTION

Modern high-speed roller bearings are exposed to demanding working conditions which approximately near the limits of materials in respect of stresses and temperatures. The operating temperature of the bearing plays a key part in the bearing reliability because it directly affects the fatigue life. To clarify the thermal performances of the bearing is quite complex and difficult because it is related to both thermal transfers and heat generation.

Considering the heat generation simulating method, Palmgren and Astridge et al. both put forward their experimental formula to predict the frictional power losses of high-speed roller bearings, in consideration of dynamic viscosity and flux of the lubricant. The method is wildly used in heat estimation of bearing and the heat generation calculated is the total power loss of the whole bearing.It leads to that it is hardly clarified the accurate position of the power loss of the bearing.

Partial power loss prediction is based on dynamic analysis of the bearing. Jones et al. presented a qusi-stastic model based on the hypothesis of pure rolling between the roller and the inner and outer rings raceways. Harris et al. developed the qusi-dynamics model, considered the elastohydrodynamic lubrication in the bearing, used the deformation compatibility condition between the roller and the ring to calculate the deformation and stress of the roller and the ring, and obtained the revolution and rotation speed of the roller. On the basis of Harris's study, Rumbarger and Poplawski et al. took interaction between cage and roller into consideration and determined the power loss generated by the contact of roller/cage and the roller/inner(outer) ring raceways contact by establishing a fluid traction moment model. Cavallaro et al. presented an analytical method to the cylindrical roller bearing with a flexible outer ring, and the structural deformation of the rings is added to operating bearing clearance correction. Leblanc et al. analyzed the roller–race contacts force in details and the structural deformations of the rings is determined. Takabi et al. researched the impact of various traction models accessible on the quai-dynamic prediction of a cylindrical rolling element bearing under radial loads.

Stein et al. estimated the thermal characteristics of ball bearing by defining three control volumes of the bearing, the rolling elements, the outer ring /housing, and the inner ring. Pouly et al. presented a thermal network method to simulate the temperatures within a thrust angular ball bearing. Takabi et al. established a thermal network composed of 17 nodes corresponding to the experimental platform and acquired the quasi-steady temperature field of the bearing varying with time. Ma et al. combined the quasi-static heat generation method with a three-dimensinal finite element model which consumes computational time for studying the thermal performance in the contact surface.

In this work,a new approach for combining a thermal network and the partial heat generation is delivered to predict the precise temperature of the bearing. The heat source is applicable to load in the accurate area of bearing parts. And a precise temperature distribution is achieved to simulation of thermal characteristics. The parameters, spindle speed, inlet lubricant temperature and flow rate, radial load are analyzed in steady states.

METHODOLOGY

PARTIAL POWER LOSS MODEL

In the study, a high-speed cylindrical roller bearing with a fixed outer ring and a inner ring guide flange is investigated. Heat is generated not only because of the friction which is affected by the speed and load in the contact surface but also due to the ring and rollers movement in the viscous lubricant. Therefore, the total power loss in the bearing is the sum of the frictional power loss and the viscous power loss. And the load and relative velocity of the components in the bearing can be obtained by solving the qusi-dynamic model(Cavallaro et al.,2005; Leblanc et al.,2009).

(1) Friction Caused Power Loss

According to the position of the friction surface, power loss in the bearing can be divided to six parts as follows.

(a) The frictional heat generation between the roller and inner ring raceway $Q_{ri}$and it between the roller and the outer ring raceway Q_{ro} can be calculated as

$$Q_{ri} = \sum_{j=1}^{N} F_{ij} V_{ij} \qquad j=1,2,3...N \tag{1}$$

$$Q_{ro} = \sum_{j=1}^{N} F_{oj} V_{oj} \qquad j=1,2,3...N \tag{2}$$

where the F_{ij}, F_{oj} are the sliding friction between the roller and the inner and outer ring raceway(Osterle, 1959) respectively, V_{ij}, V_{oj} is the corresponding relative sliding velocities and N is the total number of rollers.

(b) The frictional power loss between the roller and cage pocket is able to be calculated as

$$Q_{rc} = \sum_{j=1}^{N} \left(FC_{1j} + FC_{2j}\right) R_r \omega_{rj} \qquad j=1,2,3\ldots N \tag{3}$$

where $FC_{1j}, FC_{2j}$are the friction between the roller and the cage pocket, R_r is the radius of roller and ω_{rj} is the roller rotation angular velocity.

(c) The frictional heat generation between the guide edge of the rings and the cage can be expressed as

$$Q_{cio} = CC_i(\omega_i - \omega_m) \tag{4}$$

where CC_i is the frictional torque between the cage and the inner ring guide flange. $(\omega_i - \omega_m)$ is the relative angular velocity between the cage and the inner ring.

(d) The frictional heat generated between the roller end face and the guide edge of the rings is able to be displayed as

$$Q_{rf} = \sum_{j=1}^{N} CE_j \omega_{r_j} \qquad j=1,2,3\ldots N \tag{5}$$

where CE_j is the friction torque between the roller end face and the guide edge of the rings.

(e) The frictional heat generation between the side wall of cage pocket and the roller end face can be presented as

$$Q_{rce} = \sum_{j=1}^{N} CC_j \omega_{rj} \qquad j=1,2,3...N \tag{6}$$

where CC_j is the friction torque between each roller end face and the side wall of cage pocket.

(f) The frictional power loss between the flange and the side wall of cage pocket due to the error, eccentric eddy and gravity action in the cage manufacturing process can be expressed as

$$Q_{cio} = CC_i(\omega_i - \omega_m) + CC_o(\omega_o + \omega_m) \tag{7}$$

where CC_i,CC_o are sliding friction torque between the cage and the bearing inner/outer ring guide flanges respectively. ω_i, ω_o are the speed of inner/outer ring of bearing respectively, and ω_m is the speed of the cage.

(2) Viscous Power Loss

The churning power loss of rollers consists of the following parts

$$q_{oil} = q_{fol} + q_{rm} \tag{8}$$

where q_{fol}, q_{rm} are the churning loss caused by the drag force in the lubricating oil and the churning loss caused by its rotation, respectively.And the formula to calculate q_{rm} is shown as

$$q_{rm} = \sum_{j=1}^{N} \left(M_{fj} + M_{ej} \right) \omega_{rj} \tag{9}$$

where M_{fj}, M_{ej} are the moment of sliding friction between the circumferential face and the end face of the rolling body, respectively. ω_{rj} is the angular rotation velocity of each roller.

$$q_{fol} = \begin{cases} Z \cdot F_{OL} \cdot R_m \cdot \omega_m & k_0 = 1 \\ Z \cdot F_{OL} \cdot R_m \cdot (\omega_i - \omega_m) & k_0 = 2 \end{cases} \tag{10}$$

In Equation (10), Z means the total number of rollers, F_{OL} represents the drag force and k is a parameter related to lubrication of bearings where k0 =1 means injection lubrication and k0 =2 means under rings lubrication (Biboulet,2010).

$$q_{cm} = \left(M_{mf} + M_{me} \right) \omega_m \tag{11}$$

The equation(11) is applied to calculate the churning power loss of cage rotation. In equation(11), the moment M_{mf} and M_{me} ,which both result from fluid drag, describe the friction torque on cage pocket and the side wall of the cage pocket respectively.

Thermal loading based on the partial heat source

Fig.1(a) shows that ,in the traditional thermal analysis, the bearing is divided into three nodes, and each node represents the inner ring, outer ring and roller respectively.

Heat generation in the bearing is incapble to be loaded accurately in the corresponding frictional surface,for example, power loss located in the roller/inner ring raceways contact lack the corresponding node.In the same way, it is hard to find a node to put the effect of the roller/outer ring raceways contact in the model.And the heat generation and transfer of the cage are also omitted. Furthermore, the influence of convective heat transfer between the rolling body and the lubricating oil on the bearing temperature is ignored.

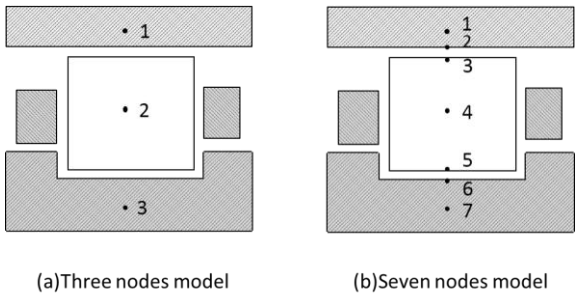

(a)Three nodes model (b)Seven nodes model

Fig. 1 Improvement on bearing nodes planning

In some proposed model, the loading of power loss between the roller and the inner and outer ring raceways is considered by setting nodes on the surface of the rolling element, as shown in Fig.1(b). Nevertheless, the heat sources induced by cage and inner ring flange as well as cage and roller are still ignored and the effect of the friction between the cage and the flange is not taken into consideration. Morever, frictional heat generation is centrally loaded in one node, which is inconsistent with the truth of the frictional contact.

In order to take these factors into account, a novel model for cylindrical roller bearing is proposed in this paper. Fig.2 illustrates the details of the model and the explanation is indicated as follows.

(a) The external structure of the bearing is properly simplified and discretized by hundreds of nodes. Inner ring including flange is divided into 144 nodes and outer ring, roller, the cage side wall, cage pocket are planned , respectively, with120,72 ,24,36 nodes.The black dots in the figure all represent the nodes in the thermal network connected with thermal resistances. Only nodes associated with load generation are numbered from1-80 including the oil inlet (node no.78), outlet (node no.80) and mist into bearing (node no.79) nodes.

(b) The frictional contact line is simplified as a series of nodes, and heat source is evenly distributed along the contact line. Also, the nodes are planed correspond one to one in the frictional surface, such as the fourth node corresponds to the 16th node. The distribution ratio of frictional heat generation in the contact area is 1:1(Burton et al.,1967).Heat flux Q_{ri} is loaded to the inner ring-roller contacts(nodes no.4-9 in the inner ring and no.16-21 in the roller) in an even way. And $Q_{ro}$is loaded to the outer ring-roller contacts which contain nodes no.66-71 in the outer ring and no.61-65 and no.43 in the roller in Fig2.

(c) Nodes no.51-61and no.21(symmetrically no.33-43 and no.16) are set to describe the heat source between the roller end face and the side wall of cage pocket Q_{rce}as well as the flange Q_{rf}. And one half of the sum of the values of $Q_{rce}$and $Q_{rf}$are distributed equally to Nodes no.51-61 and no.21(symmetrically no.33-43 and no.16).Meanwhile, nodes no.44-50 and no.22 (symmetrically nodes no.33-43 and no.16)are used to reflect the cage side wall thermal characters with loading the half of the value of Q_{rce}, which is similar to the nodes no.72-74 and no.10(symmetrically nodes no.75-77

and no.3) in inner ring flange with loading the Q_{rf}. Specifically speaking, the sum of the number of cage side wall nodes and the number of nodes on the flange is equal to the number of nodes on the corresponding surface of the roller to achieve the even heat distribution. Q_c is the heat induced by friction between the cage pocket and the roller. For the roller, nodes no.61-65 and no. 43 (symmetrically nodes no.16-21) are employed to load half of values of Q_c .Nodes no.1-3 corresponding to nodes no.13-15 in the cage are used in considering the heat source between cage and inner ring flange Q_{cio} and symmetrically nodes no.10-12 corresponding to nodes no.22-24 are loaded the heat generation in the same way.

(d) For the passage and churning power loss induced by lubricant, the no.79 is set to show the lubricant temperature in the bearing. This part of the heat generation is reflected in the temperature rise in no.79.

The energy balance method is implemented to obtain the temperature distribution of bearing. For a random node i in the thermal network, it obeys the following relationship according to the principle of heat flux balance under the condition of steady-state heat transfer without consideration of radiation.

$$\sum_{j=1}^{M}\left[F_{ji}(\mathrm{T}_j-\mathrm{T}_i)\right]+Q_{Gi}=0 \qquad \mathrm{i}=1,2,3,\ldots,\mathrm{N} \tag{12}$$

in which M is the total number of nodes having heat transfer relationship with node I, N is the total number of nodes in the whole network(N>M), and is the reciprocal of thermal resistances between i and j(any node that has a heat transfer relationship with i),and is the heat source loading in the node. For the radial and axial directions, thermal resistance coefficient is able to be calculated as (Pouly et al.,2010)

$$\Omega_1=\frac{l_1/k_1+l_2/k_2}{A} \tag{13}$$

$$\Omega_2=\frac{\ln(\mathrm{d}_2/\mathrm{d}_1)/\mathrm{k}_1+\ln(\mathrm{d}_3/\mathrm{d}_2)/\mathrm{k}_2}{2\pi l} \tag{14}$$

Where l_1,l_2 are the natural lengths and k_1,k_2 are the thermal conductivity respectively. d_1,d_2,d_3 are the diameter of a cylinder arranged in the direction in which the diameter increases.

The method to determine the convective thermal resistance can be expressed as (Brown et al.,2000)

$$h=0.0986\left\{\frac{n}{\upsilon}\left[1\pm\frac{d_0\cos(\beta)}{d_m}\right]\right\}^{1/2}k\,\mathrm{Pr}^{1/3} \tag{15}$$

where n means the rotating speed, υ is the kinematic viscosity of lubricating oil, k is the thermal conductivity of lubricant, β is the contact angle of the bearing, Pr is the Prandtl number of oil flow, d_0 is the pitch circle diameter of the bearing, and d_m is the roller diameter; and "+" means the outer ring rotates, "-" means the inner ring rotates. Considering that the convection heat transfer effect between lubricating oil and bearing is related to the different position in bearing, the convective heat transfer coefficients on the sides of the inner and outer rings were modified to 1/3 of the heat transfer coefficients at the contact surface between the inner and outer rings and rollers(Crecelius et al.,1976).And the Gauss-Jordan Elimination method is applied to solve the linear system of equations using the Fortran programming language.

Table 1 Explanations on nodes arrangement

Nodes	Explanations
43,62,63,64,65,61	Roller surface contacted with the outer ring &roller contacted with the cage pocket
16,17,18,19,20,21	Roller surface contacted with the inner ring &roller contacted with the cage pocket
36,37,38,39,40,41,42,43	Roller end face contacted with the cage slide wall
54,55,56,57,58,59	
3,75,76,77	Inner flange contacted with the roller end face
10,72,73,74	
33,34,35,16	Roller end face contacted with the flange
21,51,52,53	
15,25,26,27,28,29,30,31	Cage slide wall contacted with Roller end face
22,44,45,46,47,48,49,50	
1,2,3	Inner flange surface contacted with the cage
10,11,12	
13,14,15	Cage surface contacted with the inner flange
22,23,24	
4,5,6,7,8,9	Inner ring raceway contacted with the roller
66,67,68,69,70,71	Outer ring raceway contacted with the roller

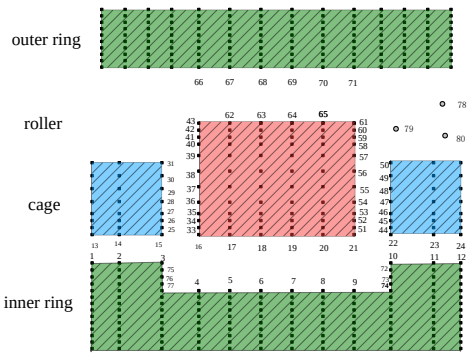

Fig. 2 Thermal network employed thermal loading

Vailidation with experiments

To verify the prediction results, an experimental equipment is set up to quantify the outer ring temperature as demonstrated in Fig3. Six temperature probes are placed evenly along the circumferential direction of the outer ring. And two temperature sensors are arranged in the inlet and outlet lubricant tubes respectively. In this experiment, the inner ring speed is increased gradually to 8000 rpm and the radial load is applied to 4kN,with the change of inlet lubricant temperature from 40℃to70℃. The bearing temperature measurement position is located on the surface of the outer ring of the bearing. There are six measuring points in the bearing, which are evenly distributed in the circumference of the outer ring. The temperature sensor is PT100 platinum resistance temperature sensor, the measurement accuracy is 2 degrees Celsius. In other words,the half width of the confidence interval U is 2℃, and normally distributed with a confidence of 95% for the inclusion factor K is 2, so the measurement uncertainty of temperature is U divided by P, which is equal to 1℃.

And the lubrication system is circulating and consists of fuel tank, heater, water cooler, oil supply pump, return pump and filter. The oil is extracted from the oil tank by the oil pump, enters the heater, heats the oil to the required inlet oil temperature, enters the tester, is extracted by the oil pump, enters the water cooler, and returns to the oil tank.

As shown in Fig 4, compared with the experimental results, partial power loss prediction model adopted in this paper shows the error of total heat generation of cylindrical roller bearings is less than 10% with the changing of the temperature of the lubricant. It can evidence that the partial power loss calculation model is convincing to some extent. With the increase of oil inlet temperature, the decrease of oil viscosity reduces the viscous friction loss of bearing fluid, so that the total heat generation of the bearing continues to decrease.

Also, a comparison of simulated and experimental results for different temperature of the lubricant is displayed in Fig5. It tends to be seen that the predicted temperatures are exceptionally near the empirical results and the error is less than 13% as the inlet lubricant temperature changes.

The induced error is because the temperature of the outer ring is influenced by both the heat generation and heat convection. The error of power loss prediction model causes the propagation of error in temperature simulation of the bearing. Meanwhile, the prediction model of convective heat transfer coefficient between the bearing and the lubricant exists error, which is needed for further research.

Fig. 3 Experiments equipment

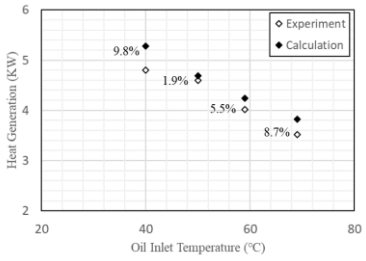

Fig. 4 Calculative heat generation compared with test value

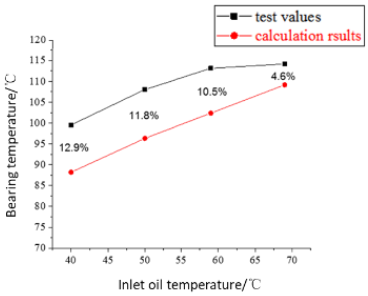

Fig. 5 Error change with inlet oil temperature

RESULTS AND DISCUSSION

The steady temperature distribution of the bearing and thermal characteristics are displayed in this chapter and the operating parameters such inner ring rotating speed, inlet lubricant temperature, lubricant flow rate and the radial load of the bearing are expressed by n,T_{oil},m and Fr respectively.

As seen in Fig. 6, the highest temperature of the bearing is 95℃, which appears in two places, which are the contact between the roller and the outer ring raceway and the contact between the guide flange of the inner ring and the cage. And

the lowest temperature of this bearing is 50℃ which is shown on the outer surface of the cage(under the condition of *Fr* = 4kN, *Toil* =40℃, *m* = 3.6L/min and *n* =8000 rpm). The temperature of the whole roller element is higher and the temperature of the side wall of the cage pocket is obviously lower than that of other elements.

It can be seen that the temperature of the contact position between the outer ring raceway and rollers is higher than that of other positions of the outer ring because of the precise loading in the outer ring raceways /roller contact. It is also shown that temperature distribution of the bearing is symmetric with respect to the middle axis in the axial direction. As mentioned in section of thermal loading, the thermal loading is completely symmetric along the axial direction of the bearing. Thus, temperature distribution has a symmetric characteristic. Fig. 6 displays that in inner ring flange/cage side wall contact, the temperature of the cage is much lower than the flange. It can be explained that bearing temperature is not only affected by the heat source loading but also by the heat convection, which is a positive correlation of the heat exchange area and convective heat transfer coefficient. And with a same heat conduction coefficient, the side wall of cage pocket is cooled by lubricant all around in comparison with the inner ring flange.In addition, the temperature gradient in the outer ring is large, so the thermal expansion of the material of the outer ring should be considered in the design of bearings.

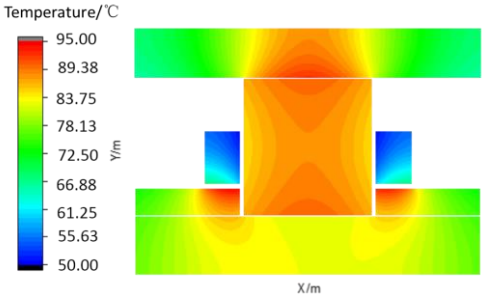

Fig. 6 Temperature distribution of bearing

Bearing temperature distribution at different inner ring rotation speed is shown in Fig. 7. With the increase of the rotation speed, the heat generation of the bearing increases, leading to the temperature of the bearing element increasing. The temperature at the contact surface between the guide flange and the cage rises sharply, while the temperature of the cage changes little due to better cooling.

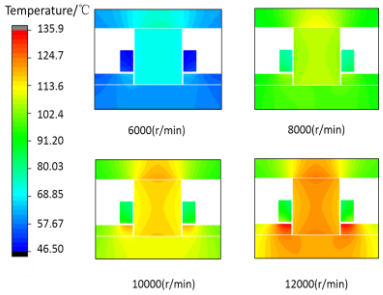

Fig. 7 Influence of rotational speed on temperature of bearing parts(Fr=4000N,Toil=70℃, m=3.6L/min）

At low rotation speed conditions, the temperature difference between the various parts of the bearing is not large, while the temperature gradient in the bearing increases at high rotation speed. For example, when the speed is 6000 rpm the maximum temperature difference in the bearing is 22.3℃, and when the speed is 12000 rpm, the maximum temperature difference rises to 43.5℃. With the increase of the rotate speed, the heat generation of the bearing increases, and the convective heat transfer coefficient between the oil and the bearing also increases, so that the bearing surface temperature drops rapidly. However, compared with the increase of convective heat transfer coefficient, the thermal conductivity coefficient does not vary much, so that the temperature difference between the high temperature area and the low temperature area in the bearing increases.

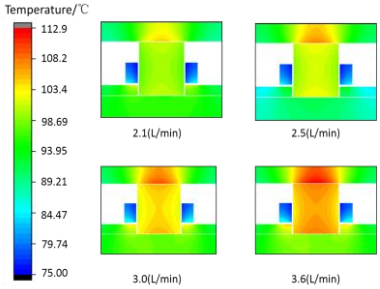

Fig. 8 Influence of inlet oil flow on temperature of bearing parts（Fr=4000N, Toil=70℃, n=8000rpm）

Fig. 8 displays the influence of inlet oil flow rate on bearing temperature field distribution. With the increase of oil flow rate, the overall temperature of the bearing increases, indicating that the heat transfer capacity improved by the increase of oil flow rate is not as obvious as the heat generation effect of the bearing due to the increase of oil flow rate. At this time, the heat generation of fluid viscous friction caused by oil is the dominant part, and the increase in oil supply is the side effect. Among them, the temperature rise of the contact position between the roller cylinder and the outer ring raceway is the most dramatic, followed by the contact place between the inner roller and the guide flange of the inner ring and the cage, while the temperature change of the cage, inner ring and other positions of the outer ring is little.

Fig. 9 presents the influence of inlet oil temperature on bearing temperature distribution. With the increase of oil temperature at the inlet, although the total heat production of the bearing decreases slightly due to the decrease of oil viscosity, the temperature of the whole bearing still increases due to the increase in oil temperature. The maximum temperature rise occurs at the contact between the rolling body and the outer ring raceway, and the temperature rise inside the rolling body is also apparent. The temperature rise in the contact between the guide flange and the cage is small.

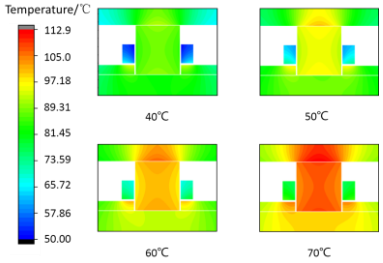

Fig. 9 Influence of inlet oil temperature on temperature of bearing parts (Fr=4000N, n=8000 rpm, m=3.6L/min)

Fig. 10 shows the influence of the radial load on bearing temperature distribution. With the increase of radial load, the overall temperature of the bearing increases very little. The roller and inner ring slip seriously with low radial load(2000N), the friction heat generation increases, resulting in the inner ring temperature is the highest in the bearing; With the increase of load, the temperature of outer ring increases sharply, while the temperature of other components changes little.

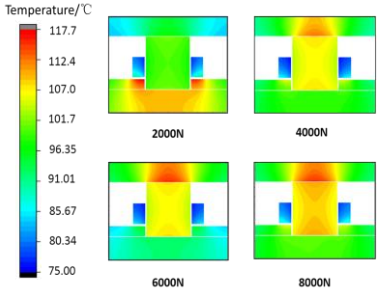

Fig. 10 Influence of radial load on temperature of bearing parts (n=8000rpm, m=3.6L/min, Toil=70℃)

CONCLUSIONS

Thermal characterics are significant variables affecting the operation of bearing. In this study, the thermal network method is combined with the partial heat generation prediction to acquire the precise temperature distribution of the cylindrical roller bearing and the computation time is saved in comparison with different simulation model.In this model,a new node distribution method is constructed in the thermal analysis. The thermal analysis model of the bearing has good calculation accuracy and reliability, among which, the error between the calculated total heat production of the bearing and the test results is less than 10%, and the error between the calculated center line temperature of the outer torus of the bearing and the test results is less than 13%. The influence of different working conditions on the distribution of the bearing temperature is studied. It is accepted that the proposed model has a higher application value to clarify the thermal performances of a cylindrical roller bearing.

REFERENCES

[1] Biboulet, N. and Houpert, L. (2010). Hydrodynamic force and moment in pure rolling lubricated contacts. part 1: line contacts. *ARCHIVE Proceedings of the Institution of Mechanical Engineers Part J Journal of Engineering Tribology* 1994-1996 (vols 208-210), 224(8), 765-775.

[2] Brown, J. R. and Forster, N. H. (2000). Operating temperatures in mist lubricated rolling element bearings for gas turbines. *Energy Conversion Engineering Conference and Exhibit*, 2000. (IECEC) 35th Intersociety. IEEE.

[3] Burton, R. A. , and Staph, H. E. (1967). Thermally activated seizure of angular contact bearings. *A S L E Transactions*, 10(4), 408-417.

[4] Cavallaro.G, Nelias, D. and Bon, F. (2005). Analysis of high-speed intershaft cylindrical roller bearing with flexible rings. *Tribology and Lubrication Technology*, 48(2), 154-164.

[5] Chi, M. , Mei, X. , Yang, J. , Liang, Z. and Hu, S. (2015). Thermal characteristics analysis and experimental study on the high-speed spindle system. *International Journal of Advanced Manufacturing Technology*, 79(1-4), 469-489.
[6] Crecelius, W. J. , and Pirvics, J. (1976). Computer Program Operation Manual on SHABERTH. A Computer Program for the Analysis of the Steady State and Transient Thermal Performance of Shaft- Bearing Systems.
[7] D Astridge and Smith, C. (1972). Heat generation in high speed cylindrical roller bearings. *ARCHIVE Proceedings of the Institution of Mechanical Engineers* 1847-1982 (vols 1-196), 83-84.
[8] Harris T. A. and Mindel, M. H. (1973). Rolling element bearing dynamics. *Wear*, 23(3), 311-337.
[9]Jones, A.B.(1960). A general theory for elastically constrained ball and radial roller bearings under arbitrary load and speed conditions. *Trans Asme*, 82(2), 309.Inst. Mech. Eng. *Elasto-hydrodynamic Lubrication Symposium*, Leeds, UK, 11–13 April 1972.
[10] Leblanc, A., Nelias, D. and C De faye. (2009). Nonlinear dynamic analysis of cylindrical roller bearing with flexible rings. *Journal of Sound & Vibration*, 325(1-2), 145-160.
[11] Osterle, J.(1959.)On the hydrodynamic lubrication of roller bearings, *Wear*, 2.
[12] Palmgren A.(1959). Ball and roller bearing engineering, 3rd ed. Philadelphia: SKF Industries Inc;
[13] Poplawski, J. V. (1972). Slip and cage forces in a high-speed roller bearing. *Journal of Lubrication Technology*, 94(2), 143-152.
[14] Pouly, F. , Changenet, C. , Ville, F. , Velex, P. and Damiens, B . (2010). Power loss predictions in high-speed rolling element bearings using thermal networks. *Tribology Transactions*, 53(6), 957-967.
[15] Rumbarger J. H., Filetti, E. G. and Gubernick, D. (1973). Gas turbine engine mainshaft roller bearing-system analysis. *Journal of Tribology*, 95(4), 401-416.
[16] Stein, J. L. and Tu, J. F. (1994). A state-space model for monitoring thermally induced preload in anti-friction spindle bearings of high-speed machine tools. *Journal of Dynamic Systems Measurement & Control*, 116(3), 372-386.
[17] Takabi, J. and Khonsari, M. M. (2014). On the influence of traction coefficient on the cage angular velocity in roller bearings. *Tribology Transactions*, 57(5), 793-805.
[18] Takabi, J. and Khonsari, M. M. (2016). On the thermally-induced failure of rolling element bearings. *Tribology International*, 94, 661-674.